The Design of Microstrip Six-Pole Quasi-Elliptic Filter with Linear Phase Response Using Extracted-Pole Technique

Kenneth S. K. Yeo, Michael J. Lancaster, *Member, IEEE*, and Jia-Sheng Hong, *Member, IEEE*

***Abstract*—The development of microstrip filters has been in great demand due to the rapid growth of wireless communication systems in this decade. Quasi-elliptic response filters are very popular in communication systems because of their high selectivity, which is introduced by a pair of transmission zeros. A number of ways of implementing the quasi-elliptic response filter on microstrip have been studied over the last two decades, i.e., the cascaded quadruplet filter, canonical filter, and extracted-pole filter. However, there is very little information in the literature giving the design details for microstrip extracted-pole filters. In this paper, design equations of the extracted-pole filter for microstrip are reviewed. A new class of microstrip filter is also presented here. This class of filter will have a quasi-elliptic function response and at the same time linear phase in the passband. The linear phase of the filter is introduced by an in-phase cross coupling, while the transmission zero is realized using an extracted-pole technique. Experimental results, together with a theoretical comparison between the group delay of this design, and the conventional quasi-elliptic six-pole filter are also presented.**

***Index Terms*—Author, please supply index terms. E-mail keywords@ieee.org for information.**

I. Introduction

THE rapid growth of wireless and mobile communications in this decade has catalyzed an increasing demand for a high-performance microstrip bandpass filter with high selectivity and linear phase or flat group delay in the passband. High-selectivity bandpass filters have been successfully achieved by introducing additional out-of-phase cross couplings in the filter structure—namely, the canonical filters [1] and cascade quadruplet (CQ) filters [2]. Conventionally, linear phase is usually achieved by a reflection-type equalizer attached via a circulator to the output of the bandpass filter. Jokela [1] has shown that by using the canonical filter structure, both high selectivity and linear phase is achievable without an external equalizer. However, there are some disadvantages attached to the canonical structure. The cross couplings, both in-phase and out-of-phase, contribute to the transmission zeros both at real and imaginary axes. Therefore, canonical filters are very difficult to tune, which is potentially difficult for narrow-band bandpass filters. In Jokela's design, as shown in Fig. 1(a), three types of resonator topologies are used to realize the required cross coupling. For a single topology filter, it is always difficult to arrange the resonators in order to achieve both in-phase and out-of-phase cross couplings. For CQ filters, both high selectivity and linear phase can be achieved. CQ filters have more flexibility compared to the canonical filter because the transmission zero pair at the imaginary axis (real frequency) is controlled by an out-of-phase cross coupling and the real axis (imaginary frequency) is controlled by an in-phase cross-coupling independently. However, to achieve both real and imaginary frequency transmission zero pairs, a minimum of eighth order is required due to the arrangement of the CQ filter.

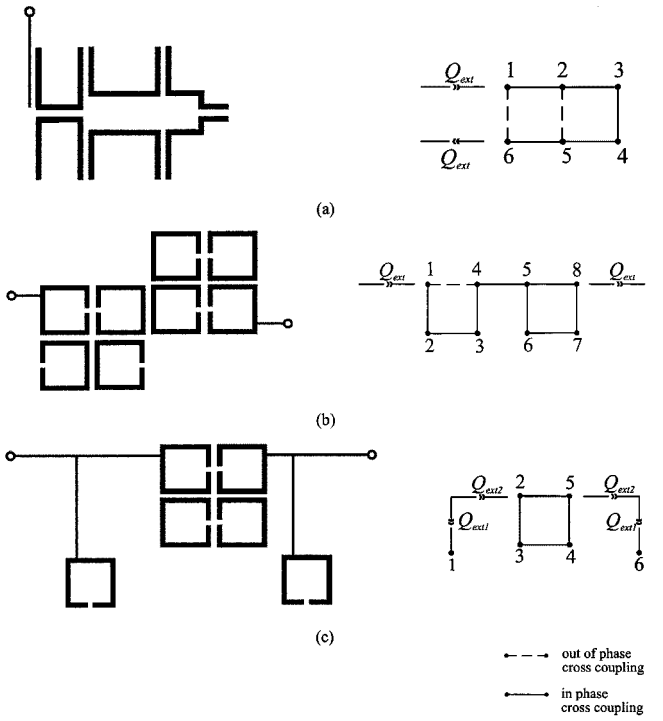

Fig. 1. Coupling structure and microstrip implementations for: (a) canonical filter, (b) cascaded quadruplet filter, and (c) extracted-pole filter.

In this paper, a new way to achieve both high selectivity and linear phase in the passband for microstrip filters is proposed. The structure allows for a sixth-order minimum. This new structure originated from TE_{011}-mode waveguide filters [3]. The transmission zero pair at the imaginary axis is extracted from the transfer function and realized separately with a pair of bandstop filters and phase shifters connected to the end of the main coupling structure. The real axis transmission zero, which flattens

Manuscript received August 24, 1999.

The authors are with the School of Electronic and Electrical Engineering, University of Birmingham, Edgbaston, Birmingham B15 2TT, U.K.

Publisher Item Identifier S 0018-9480(01)01072-9.

the group delay, is achieved by an in-phase cross coupling. Thus, the real and imaginary zero pairs are independently tuned. This has made the structure very attractive for practical design. This design can be achieved even for resonator topology, which can only realize single type of coupling. The microstrip (or stripline) layout of the canonical, CQ, and extracted-pole filters are shown in Fig. 1, together with the coupling configuration diagrams.

The extracted pole for microstrip was introduced by Hedges and Humphreys [4] by using microstrip hairpin topology. They demonstrated that the extracted-pole technique developed by Rhodes [3] can be transferred to microstrip using a four-pole bandpass filter. However, there was little information on how to obtain the parameters for the microstrip design from the extracted-pole synthesis. This paper will extend Rhodes' extracted-pole technique to microstrip by working through an example of a six-pole quasi-elliptic response filter. A new set of equations for determining the external Q-factor and coupling coefficients are reviewed. These equations will depend on the bandpass parameters instead of the low-pass parameters, which are usually used in most filter designs. A circuit model for the microstrip extracted-pole filter will also be reviewed. The comparison between the theoretical quasi-elliptic function response and the approximated circuit model will be discussed.

A six-pole microstrip bandpass filter has been successfully designed and made in copper microstrip with duroid substrate $(\varepsilon_r = 10.8)$ with the assistance of circuit model simulation and full-wave electromagnetic (EM) simulation [5]. The design consideration and experimental results will be presented. The results of the six-pole microstrip filter, together with its group delay response, will also be presented.

II. Extracted-Pole Synthesis

A brief summary of the extracted-pole synthesis will be outlined here. A detailed analysis of the extracted-pole synthesis can be found in [3]. The synthesis starts from the low-pass quasi-elliptic transfer function. The extracted-pole synthesis can only be performed on a complex conjugate symmetrical network. Therefore, it will only work on an even-order transfer function with a fourth-order minimum.

The initial cycles of the extracted-pole synthesis involve extracting a unity impedance phase shifter from both ends of the network with complex conjugate symmetry. The next cycle is to extract a complementary pair of the complex axis transmission zeros (real frequency zeros) from each side of the passband by extracting a shunt resonator from both ends of the remaining network. This process will be repeated until all complex zeros are extracted from the transfer function. The remaining network can then be extracted using a cascade synthesis.

III. Microstrip Realization

After performing the extracted-pole synthesis, a set of parameters will be obtained that corresponds to the low-pass prototype, as shown in Fig. 2. The square blocks with symbols ψ_1 and $-\psi_1$ represent phase shifters with phase shift of ψ_1 and $(180° - \psi_1)$, respectively, and the block with symbols "J_m" and "1" are J_m admittance inverters and unity admittance inverters, respectively. The symbols B_{LPm} and C_{LPm} are the frequency

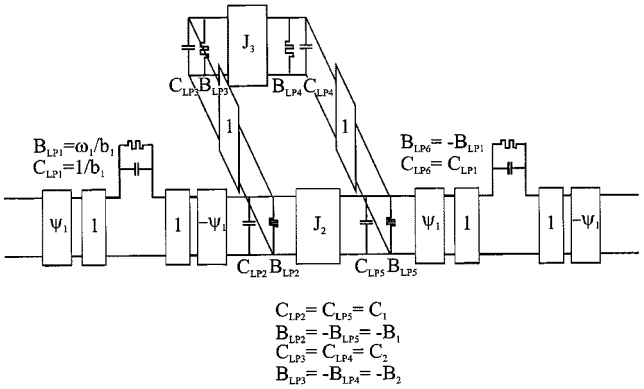

Fig. 2. Low-pass block diagram of an extracted-pole quasi-elliptic response filter with linear phase.

invariant admittances and the capacitances, respectively. This low-pass prototype can be transformed into a bandpass filter by using the following transformation equations [6]:

$$C_{BPm} = \frac{1}{\omega_o}\left(\frac{C_{LPm}}{\Delta} + \frac{B_{LPm}}{2}\right) \tag{1}$$

$$L_{BPm} = \frac{1}{\omega_o\left(\dfrac{C_{LPm}}{\Delta} - \dfrac{B_{LPm}}{2}\right)} \tag{2}$$

where ω_o is the center frequency and Δ is the fractional bandwidth of the bandpass filter. The frequency invariant admittance B_{LP} is absorbed into the capacitance and inductance in the transformation because it cannot be realized in a real circuit. Thus, the resonator is detuned from the center frequency f_o. From (1) and (2), it is obvious that all the resonators are resonating at different frequencies. Therefore, this type of filter is not a synchronously tuned filter.

The circuit shown in Fig. 2 is not easily realized using microstrip because of the series resonator in the extracted section. Fig. 3(b) shows a small modification of the extracted section of the filter [see Fig. 3(a)] so that it can be easily realized using a microstrip resonator (for this case, it is a square-loop resonator [2]), as shown in Fig. 3(c). This modification is verified by comparing the frequency responses of the two circuits, as shown in Fig. 4. These responses are obtained using the Hewlett-Packard Advanced Design System (ADS) circuit model simulator [7]. This has shown that the modification gives a very good approximation.

The full-circuit model for the microstrip extracted-pole filter is shown in Fig. 5. The admittance inverters are realized using a π-network of capacitors. To convert the circuit model of Fig. 5 into microstrip, the coupling between the resonator and feed line (the external Q-factor) and the coupling between resonators (coupling coefficient) have to be determined. A new set of the external Q-factor equations, i.e., $Q_{\text{ext},m}$ and the coupling coefficients $M_{m,m+1}$, is derived for the microstrip extracted-pole filter and is given as

$$Q_{\text{ext},m} = Q_{\text{ext},n-m} = \omega_m C_{BPm}, \qquad m = 1, 2 \tag{3}$$

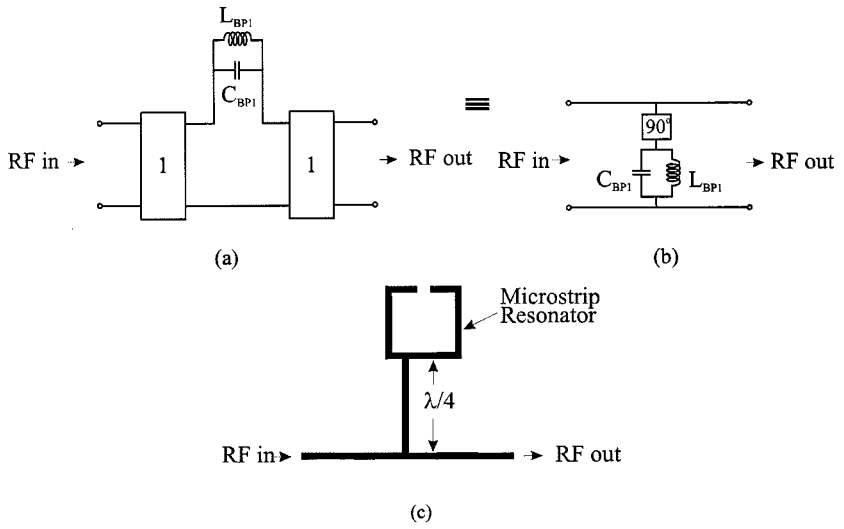

Fig. 3. Extracted section of the filter. (a) Original extracted section. (b) Modified extracted section to a realizable circuit model. (c) Equivalent circuit for microstrip layout using a square-loop resonator.

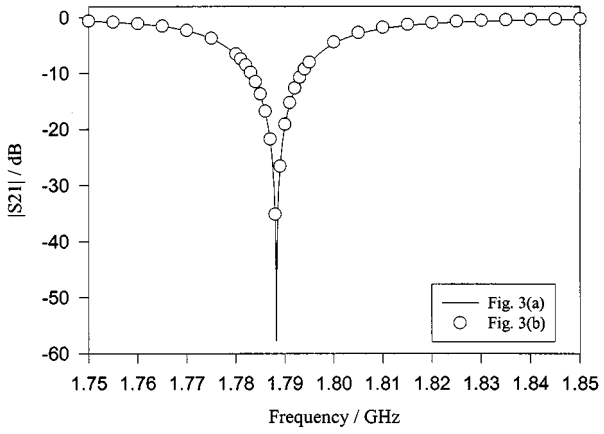

Fig. 4. Plot of $|S21|$ of the modified extracted section compared to the original circuit.

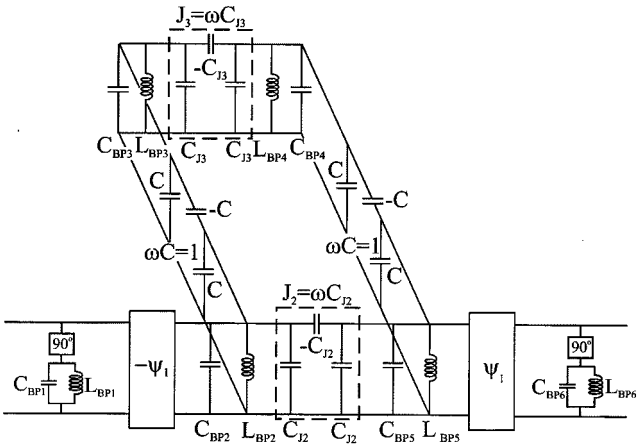

Fig. 5. Full-circuit model for the bandpass extracted-pole microstrip filter.

$$M_{m,m+1} = M_{n-m,\,n-m+1} = \sqrt[4]{\frac{L_{BPm}L_{BPm+1}}{C_{BPm}C_{BPm+1}}}, \quad m = 2 \text{ to } \left(\frac{n}{2} - 1\right) \tag{4}$$

$$M_{m,m+1} = J_m \sqrt[4]{\frac{L_{BPm}L_{BPm+1}}{C_{BPm}C_{BPm+1}}}, \qquad m = \frac{n}{2} \tag{5}$$

$$M_{m-1,\,m+2} = J_{m-1} \sqrt[4]{\frac{L_{BPm-1}L_{LPm+2}}{C_{BPm-1}C_{BPm+2}}}, \qquad m = \frac{n}{2} \tag{6}$$

where n = the number of poles, $\omega_m = 2\pi f_m$, and f_m is the resonance frequency of the mth resonator. Conventionally, the low-pass parameters [8] are used to determine the external Q-factors and the coupling coefficients. However, the bandpass parameters are used here because the extracted-pole filter is not a synchronously tuned filter. If the low-pass parameters were used, the external Q-factors and coupling coefficients would not be perfectly accurate. This is because the conventional equations for determining external Q-factors and the coupling coefficients do not include the frequency invariant admittances, which are introduced by the extracted-pole synthesis.

IV. Example on Six-Pole Quasi-Elliptic Function

As an example, a six-pole quasi-elliptic function filter with a passband return loss of 20 dB, a real frequency transmission zero pair at $p = \pm j1.414$, and an imaginary frequency transmission zero pair at $p = \pm 0.953076$ will be used. This example is taken from Rhodes' paper [3]. The extracted-pole synthesis will not be repeated here since it was thoroughly explained in [3]. Here, only the results from the extracted synthesis will be quoted and shown in Table I.

The six-pole bandpass filter example has the following specifications:

- center frequency: 1842 MHz;
- fractional bandwidth: 4.07%.

The capacitance, inductance, and resonant frequency for each of the resonators can be determined by applying transformation equations (1) and (2), and are shown in Table II.

TABLE I

Phase shift, φ_i / °	Transmission Zero, Ω_i	Residue, b_i
52.3531	1.414	0.871402

m	Capacitance, C_{Lm}	Susceptance, B_{Lm}	Admittance Inverter, J_m
1	1.14757	1.622672	Not Applicable
2	2.20593	0.779383	-0.38215
3	1.07194	0.0271943	-0.493517

TABLE II

m	Capacitance, C_{Am}/nF	Inductance, L_{Am}/pH	Resonant Frequency, f_o/GHz
1	2.50533	3.15650	1.790
2	4.64746	1.58343	1.855
3	2.27355	3.28025	1.843
4	2.27590	3.28364	1.841
5	4.71480	1.60637	1.829
6	2.36513	2.97986	1.896

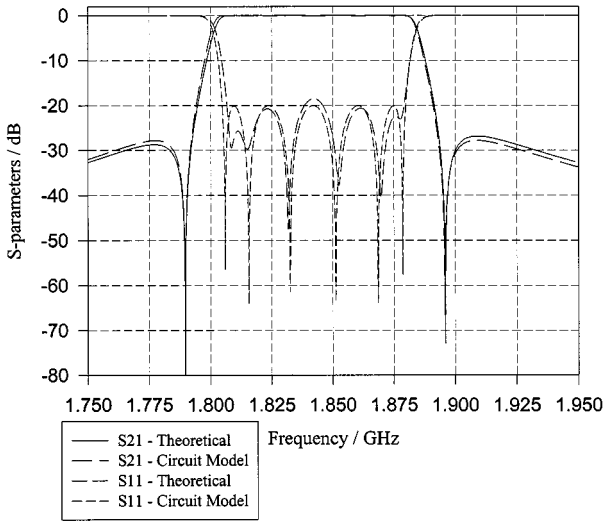

Fig. 6. Theoretical responses together with the circuit model simulation results.

The coupling coefficients and the external Q-factors of this bandpass filter can be determined from (3)–(5) and their values are given as

$$M_{23} = M_{45} = 0.02648$$
$$Q_{\text{ext1}} = Q_{\text{ext6}} = 28.17279$$
$$M_{34} = 0.01875$$
$$Q_{\text{ext2}} = Q_{\text{ext5}} = 54.17624$$
$$M_{25} = 7.07229 \times 10^{-3}.$$

A circuit model simulation is performed using an ADS simulator [7] with the parameters determined above. Fig. 6 shows the simulation results and the theoretical response of the sixth-order quasi-elliptic function. This shows that the circuit model gives

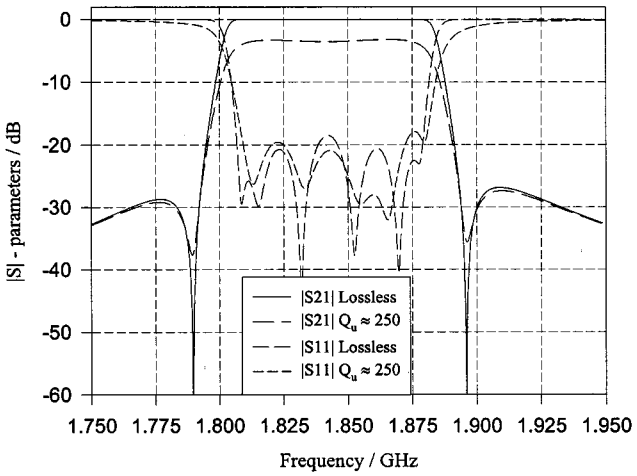

(a)

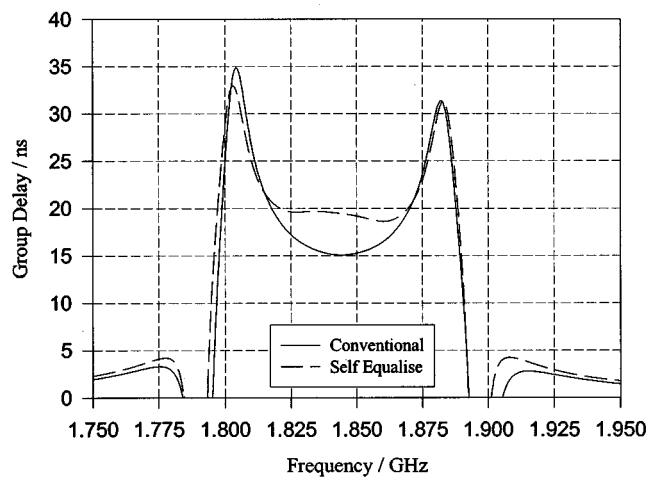

(b)

Fig. 7. (a) Circuit model simulation responses for six-pole quasi-elliptic response filter for lossless and with unloaded Q of about 250. (b) Comparison between the group delay for conventional quasi-elliptic and self-equalized quasi-elliptic function filter.

a very good approximation of the six-pole quasi-elliptic function. However, there are some errors in the passband ripples in the circuit model. This can be accounted for by the frequency variant admittance inverters used in the circuit model, whereas the theoretical admittance inverters from the extracted-pole synthesis are frequency invariant. The frequency variant admittance inverters are used in the circuit model because they give a better approximation of the real microstrip coupling structures.

Loss can be added to the circuit model to simulate the conductor loss of the real filter by adding parallel resistances to the parallel *LC* resonators. Fig. 7(a) shows the responses of a circuit model with added losses of unloaded Q-factor of 250 and the ideal case. When the loss is added, the passband insertion loss will increase to about 3 dB. To illustrate the linear phase response of this filter, a comparison is made between a conventional six-pole quasi-elliptic filter (without in-phase cross coupling) and this example. It is clearly shown in Fig. 7(b) that by

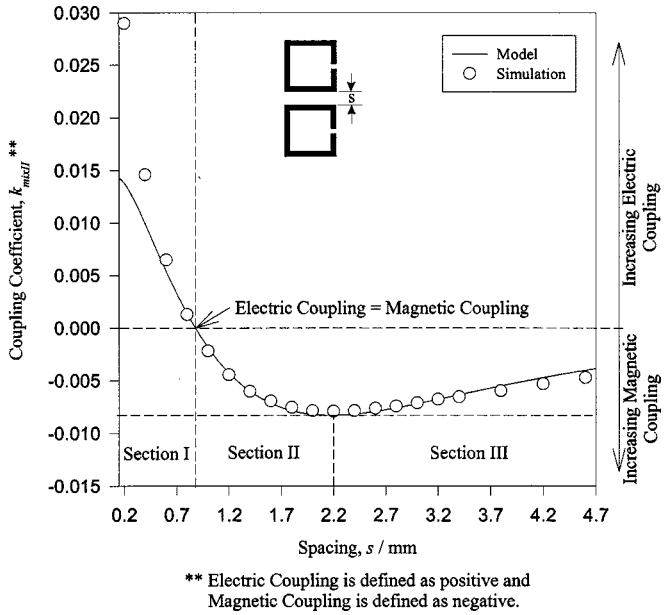

Fig. 8. Plot of type-II mixed coupling of a square open-loop resonator.

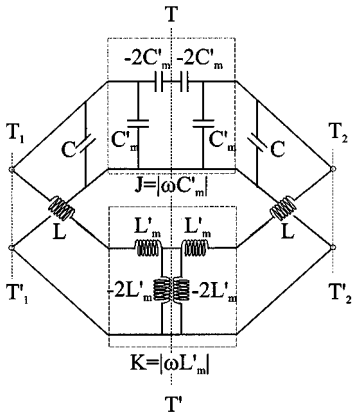

Fig. 9. Circuit model of the type-II mixed coupling.

introducing an in-phase cross coupling, the group delay can be flattened significantly. By introducing the in-phase cross coupling, type-II mixed coupling is introduced.

V. Type-II Mixed Coupling

The type-II mixed coupling was first discussed by Hong *et al.* [9] for a microstrip hairpin structure. This type of coupling is not continuously decreasing with coupling distance, but increasing until one particular point then starts decreasing. Here, there are actually two types of coupling existing in the type-II mixed coupling. Fig. 8 shows a plot of the coupling coefficients, which are obtained from full EM [5] simulation, against the coupling distance for the microstrip square-loop resonators. The type-II mixed coupling is also the superposition of the electric and magnetic couplings, as in the type-I mixed coupling [2]. However, the magnetic coupling of the type-II mixed coupling is out-of-phase with respect to the electric coupling. This is in contract to the type-I mixed coupling where the magnetic coupling is in-phase with respect to the electric coupling. Therefore, the electric and magnetic couplings in type-I mixed coupling enhance each other, whereas the electric and magnetic couplings of the type-II mixed coupling cancel out each other.

When the resonators are placed very close to each other, the electric coupling dominates. The electric couplings are very strong, but decay very rapidly. At one particular spacing, i.e., about 0.9 mm for this case, there is no coupling between the two resonators. This is because the electric coupling is equal to the magnetic coupling. In Fig. 8, marked "Section II," the coupling increases with increasing coupling distance, which is not expected in most coupling structures. This happens because the net coupling has changed from electric to magnetic, and also because the magnetic couplings decay at a slower rate compared to the electric coupling. Therefore, the net magnetic coupling appears to be increasing (more negative). The couplings will increase until one particular point and start decreasing again, as shown in Fig. 8, marked "Section III."

When the spacing between the resonators is very far apart, the electric fields between the resonators are negligible. Therefore, the coupling appears to be purely magnetic.

To model the type-II mixed coupling, a circuit diagram, as shown in Fig. 9, is used. Due to the arrangement of the coupling structure, the flow of currents in the two resonators is changed compared to the type-I mixed coupling [2]. This will cause the mutual inductances L_m in the circuit model to change from positive to negative and vice versa. The mutual capacitances C_m remain the same because they are independence of current. By inserting a short circuit (electric wall) and open circuit (magnetic wall) along the $T-T'$-plane, the resonant frequency of the of the circuit can be determined as [2]

$$f_e = \frac{1}{2\pi\sqrt{(C-C_m)(L+L_m)}} \tag{7}$$

$$f_m = \frac{1}{2\pi\sqrt{(C+C_m)(L-L_m)}}. \tag{8}$$

The coupling coefficient of the type-II mixed coupling can be determined using the following:

$$k_{\text{mixII}} = \frac{f_e^2 - f_m^2}{f_e^2 + f_m^2} = \frac{C_m L - C L_m}{CL - C_m L_m}. \tag{9}$$

Assuming that $C_m L_m \ll CL$, which is usually the case, (9) can be simplified to

$$k_{\text{mixII}} \approx \frac{C_m}{C} + \left(-\frac{L_m}{L}\right) = k_E + (-k_M) \tag{10}$$

where k_E is the electric coupling and k_M is the magnetic coupling. The negative sign in (10) indicates that the magnetic coupling is out-of-phase with respect to the electric coupling. Using Hong's model [2] for the electric coupling k_e and magnetic coupling k_m of the square-loop resonators, it is shown that the type-II mixed coupling model fits reasonably well when the spacing between the coupling resonators is greater than 0.3 mm,

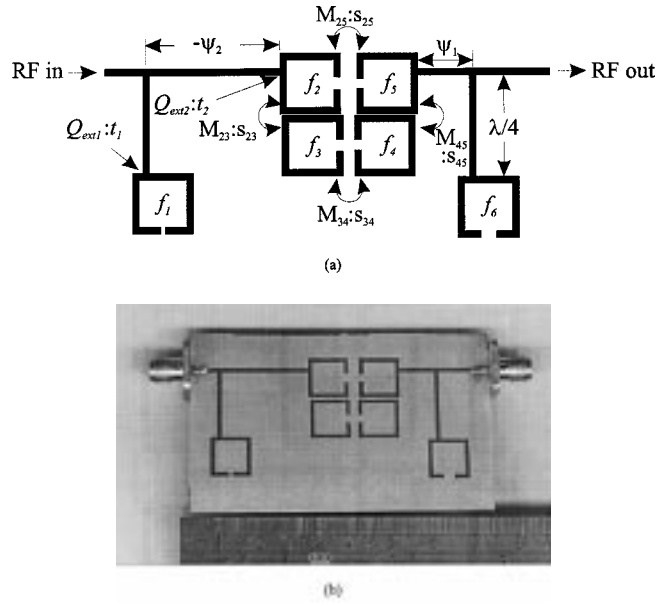

Fig. 10 (a) Microstrip circuit layout of an extracted-pole bandpass quasi-elliptic response filter with linear phase with square-loop resonators. (b) Photograph of the fabricated filter.

TABLE III

External Q-factor	Coupling Spaces
$t_1 = 1.55$ mm	$s_{12} = s_{56} = 0.25$ mm
$t_2 = 2.40$ mm	$s_{23} = 1.70$ mm
	$s_{34} = 2.40$ mm

as shown in Fig. 8. The best fit obtained when the ratio between the electric coupling and the magnetic coupling are 0.6–0.4, i.e.,

$$k_{\text{mixII}} = 0.6k_e - 0.4k_m. \tag{11}$$

VI. Experimental Filter

The layout of the six-pole microstrip filter using square-loop topology is shown in Fig. 10(a). A photograph of the fabricated filter is shown in Fig. 10(b). Here, ψ_1 and $(180^\circ - \psi_1)$ are the electrical length of the microstrip transmission lines. The spacing between the resonators is determined using full EM [5] simulation. The physical dimensions for the couplings and external Q-factors corresponding to Fig. 10(a) are shown in Table III.

This filter is fabricated using copper microstrip on an RT/Duriod substrate with relative dielectric constant ε_r of 10.8 and thickness of 1.27 mm. The linewidth of the microstrip is 1.1 mm throughout. The measured performance of the fabricated microstrip filter, which is obtained using the HP8720 network analyzer, is shown in Fig. 11(a). Some tuning is performed in this measured result to obtain the best response. The tuning is achieved by placing small dielectric materials at the appropriate position to change the resonant frequencies of each resonator accordingly. Tuning is essential because of the unavoidable fabrication errors. The midband insertion loss is measured at about 3.3 dB, which is mainly contributed by the conductor loss of the copper. Two attenuation poles at the rolloff frequency near the passband, which improve selectivity, are achieved. The measured group delays are shown in Fig. 11(b). The group delay of the experimental results is slightly lower compared to the predicted circuit model because there are slight increases in the bandwidth of the fabricated filter.

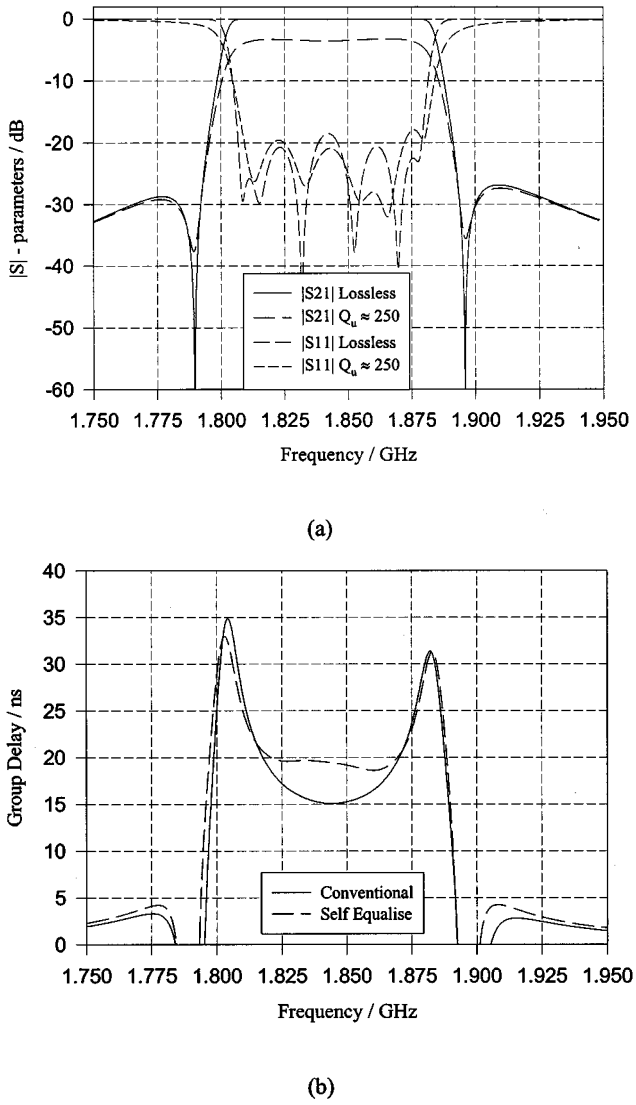

Fig. 11. (a) Experimental results for $|S11|$ and $|S21|$. (b) Comparison between the experimental and theoretical group delay.

VII. Conclusion

We have presented the design procedure for the extracted-pole technique for microstrip filter. A circuit model of the microstrip extracted pole is also presented. This model has shown close correlation with the theory. This model makes the design of microstrip extracted-pole technique for quasi-elliptic function filter more straightforward. To demonstrate the validity of the circuit model, a six-pole quasi-elliptic microstrip filter has been designed, fabricated, and tested. The measurement circuit model, together with the theoretical response, has been presented. We have also shown that by introducing an in-phase cross coupling in the microstrip extracted-pole filter, a linear

phase filter with a real transmission zero pair can be achieved. The unexpected phenomena of the type-II mixed coupling has been discussed. A circuit model is also presented to explain these phenomena.

REFERENCES

[1] K. T. Jokela, "Narrow-band stripline or microstrip filters with transmission zeros at real and imaginary frequencies," *IEEE Trans. Microwave Theory Tech.*, vol. MTT-28, pp. 542–547, 1980.

[2] J. S. Hong and M. Lancaster, "Couplings of microstrip square open-loop resonators for cross-coupled planar microwave filters," *IEEE Trans. Microwave Theory Tech.*, vol. 44, pp. 2099–2109, Nov. 1996.

[3] J. D. Rhodes and R. J. Cameron, "General extracted pole synthesis technique with applications to low-loss TE_{011} mode filters," *IEEE Trans. Microwave Theory Tech.*, vol. MTT-28, pp. 1018–1028, 1980.

[4] S. J. Hedges and R. G. Humphreys, "An extracted pole microstrip elliptic function filter using high temperature superconductors," in *Proc. EuMC*, 1994, pp. 517–521.

[5] *EM User's Manual*, Sonnet Software Inc., Liverpool, NY, 1993.

[6] J. D. Rhodes, *Theory of Electrical Filters*. New York: Wiley, 1976.

[7] *ADS Manual*, Hewlett-Packard Company, Santa Rosa, CA, 1990.

[8] G. Matthaei, L. Young, and E. M. T. Jones, *Microwave Filters, Impedance-Matching Networks, And Coupling Structures*. Norwood, MA: Artech House, 1964.

[9] J. S. Hong and M. J. Lancaster, "Cross-coupled microstrip hairpin-resonator filters," *IEEE Trans. Microwave Theory Tech.*, vol. 46, pp. 118–122, Jan. 1998.

Kenneth S. K. Yeo received the B.Eng. degree (with honours) in electronic and communication engineering and the Ph.D. degree from Birmingham University, Edgbaston, Birmingham, U.K., in 1996 and 2000, respectively. He doctoral research concerned high-temperature superconducting microwave devices.

From 1996 to 2000, he was a graduate member of the School of Electronic and Electrical Engineering, Birmingham University, where he was also a Graduate Teaching Assistant. He is currently a Research Fellow in the Communication Engineering (CE) Group and the Electronic Materials and Devices Research (EMD) Group, Birmingham University. His current research interests include high-temperature superconductor applications, microwave devices, microwave filters, microwave ferrite devices, and agile micromachined devices.

Michael J. Lancaster (M'91) received the engineering degree in physics and the Ph.D. degree from Bath University, Bath, U.K., in 1980 and 1984, respectively. His doctoral research concerned nonlinear underwater acoustics.

Upon leaving Bath University, he joined the Surface Acoustic Wave (SAW) Group, Department of Engineering Science, Oxford University, as a Research Fellow, where his research concerned the design of new novel SAW devices, including filters and filter banks. These devices worked in the 10-MHz–1-GHz frequency range. In 1987, he became a Lecturer in the School of Electronic and Electrical Engineering, University of Birmingham, Edgbaston, Birmingham, U.K., where he lectured in EM theory and microwave engineering. Shortly upon joining the University of Birmingham, he began the study of the science and applications of high-temperature superconductors, involved mainly at microwave frequencies. He currently heads the Electronic and Materials Devices Group, University of Birmingham, as a Reader. His current personal research interests include microwave filters and antennas, as well as the high-frequency properties and applications of a number of novel and diverse materials.

Dr. Lancaster currently serves on the IEEE Microwave Theory and Techniques Society (IEEE MTT-S) International Microwave Symposium Technical Committee.

Jia-Sheng Hong (M'94) received the D.Phil. degree in engineering science from Oxford University, Oxford, U.K., in 1994.

From 1979 to 1983, he was a Teaching/Research Assistant in radio engineering with Fuzhou University. In 1983, he was a Visiting Researcher at Karlsruhe University, Karlsruhe, Germany, where he was involved with microwave and millimeter-wave techniques from 1984 to 1985. In 1986, he returned to Fuzhou University, as a Lecturer in microwave communications. In 1990, he became a graduate member of St. Peter's College, Oxford University, where he conducted research in EM theory and applications. Since 1994, he has been a Research Fellow at Birmingham University, Edgbaston, Birmingham, U.K. His current interests include RF and microwave devices for communications, microwave filters and antennas, microwave applications of high-temperature superconductors, EM modeling, and circuit optimization.

Dr. Hong was the recipient of a 1983 Friedrich Ebert Scholarship. He was also awarded a 1990 K. C. Wong Scholarship by Oxford University.